

LETTER • OPEN ACCESS

Population ageing determines changes in heat vulnerability to future warming

To cite this article: Chang-Eui Park *et al* 2020 *Environ. Res. Lett.* **15** 114043

View the [article online](#) for updates and enhancements.

Environmental Research Letters



LETTER

OPEN ACCESS

RECEIVED
23 June 2020

REVISED
27 August 2020

ACCEPTED FOR PUBLICATION
1 October 2020

PUBLISHED
25 November 2020

Original content from
this work may be used
under the terms of the
[Creative Commons
Attribution 4.0 licence](#).

Any further distribution
of this work must
maintain attribution to
the author(s) and the title
of the work, journal
citation and DOI.



Population ageing determines changes in heat vulnerability to future warming

Chang-Eui Park^{1,2} , Sujong Jeong^{1,2,6} , Luke J Harrington³ , Myong-In Lee⁴ and Chunmiao Zheng⁵

¹ Department of Environmental Planning, Graduate School of Environmental Studies, Seoul National University, Seoul, Republic of Korea

² Environmental Planning Institute, Seoul National University, Seoul, Republic of Korea

³ Environmental Change Institute, University of Oxford, Oxford, United Kingdom

⁴ School of Urban and Environmental Engineering, UNIST, Ulsan, Republic of Korea

⁵ School of Environmental Science and Engineering, Southern University of Science and Technology (SUSTech), Shenzhen, People's Republic of China

E-mail: sujong@snu.ac.kr

Keywords: population ageing, unprecedented hot summers, heat exposure, climate change, Shared Socio-economic Pathways

Supplementary material for this article is available [online](#)

Abstract

Population ageing, an increase in the older age group's portion of the total population, worsens the heat tolerance of a society. However, impacts of ageing on the social exposure to projected unprecedented hot summers (UHSs) are uncertain. We show that a shifting of the population distribution towards older ages amplifies the vulnerability of a country to the increasing frequency of UHSs as a result of warming during 2040–2070, especially in most populated regions such as China, India, and sub-Saharan countries. The warming scenarios from Representative Concentration Pathway (RCP) 8.5 are combined with population scenarios from three Shared Socio-economic Pathways (SSPs) SSP2, SSP3, and SSP5 together to estimate the exposure to UHSs. The ageing-driven increase in the exposure of elderly to UHSs ranges 51–198, 91–261, and 47–156 million in China, India, and sub-Saharan countries, respectively, between population scenarios. In China, with decreasing total population, the exposure to UHSs will be increased by rapid population ageing. In India and sub-Saharan countries, the potential of ageing to raise the exposure to UHSs will be even larger than that of warming. In contrast, in aged societies with slow ageing trend, e.g. United States and Europe, the warming mainly increases the exposure to UHSs. Our results suggest the changing age structure could exacerbate a country's heat vulnerability despite limiting warming to a certain level in the future.

1. Introduction

Population ageing is one of the most significant contributors to world population change (Baccini *et al* 2011, Basu 2009, World Health Organization (WHO) 2015a, Li *et al* 2016, United Nations 2019a). Developed countries are entering the aged society due to the decrease in mortality and fertility rates (United Nations 2019b). The population aged 65 years and above (P65+) in the United States (US) in 2014 was 46 million, which is twice that in any year in the 1960s (Mather *et al* 2015). As a result, the share of P65+ to total population reaches 15% in 2014 in

the US, which is larger than that in 1960s by 6% (Mather *et al* 2015). In Germany, the share of the P65+ reached 21.1% of the total population in 2016, which was larger than that in 1996 by 5.5% (Statistical Office of the European communities 1990). In the future, the number of elderly will rapidly increase in highly populated countries with middle- and low-incomes (World Health Organization (WHO) 2011, United Nations 2019b). In China, the population aged 60 years and beyond (P60+) is projected to account for 28% of total population in 2040, which is more than twice the fraction in 2010 (World Health Organization (WHO) 2015b). The percentage of P60+ in India will exceed 10% of the total population in the 2020s, which will further increase by 10%

⁶ Author to whom any correspondence should be addressed.

in the 2060s (World Health Organization (WHO) 2015a). As a result of worldwide ageing, one of six people in the world will be aged 65 years or above in 2050 (United Nations 2019b).

The projected growth in the population of the elderly poses a serious danger to public health under a given warming scenario (World Health Organization (WHO) 2015a, Arnell *et al* 2016). Elderly people are much more vulnerable to heat stress in conjunction with their low adaptability to hot weather through factors, such as reduced sweat gland output, reduced skin blood flow, and smaller increase in cardiac output (Kenney and Munce 2003, Guo *et al* 2017). The high possibility of living alone, physical inactivity, having chronic diseases, and using of medications also increases heat-related mortality of the elderly (Hajat *et al* 2010, Guo *et al* 2017). The susceptibility of the elderly to heat stress has been reported when historically extreme heat events occur during previous record-breaking hot summers (Larrieu *et al* 2008, Dole *et al* 2011, Yiou *et al* 2020). During the 2003 summer for example—one of the hottest summers in Europe—the heat wave-induced deaths in France were mostly among the elderly (Larrieu *et al* 2008). According to the ageing trend in recent decades, more elderly persons have been exposed to extreme heat waves occurred in the record-breaking hot summers (Urban *et al* 2017, 2020). Further, the accelerated ageing trend in future will increase the exposure of elderly to projected unprecedented hot summers (UHSs), defined as hotter summer than the hottest summer in historical record, accompanied by strong heat waves (Jones *et al* 2015, King 2017, Harrington and Friederike 2018). Thus, there is a need to investigate the ageing-driven change in the elderly population exposed to UHSs for future climates to aid decision-makers in reducing hot-weather-induced damages on public health.

This study aims to quantify the importance of ageing with reference to the increase in the exposure of older persons to unprecedented future heat in six regions with large populations, namely, China, India, sub-Saharan countries with low-incomes (SSA-L), Brazil, US, and the 15 countries that joined the European Union prior to 2004 (EU15) during the mid-21st century. The change in P_{65+UHS} is computed based on the combination climate change projections of 27 global climate models (GCMs) under the Representative Concentration Pathway 8.5 (RCP8.5) scenario in combination with three population scenarios following Shared Socio-economic Pathways (SSPs) SSP2, SSP3, and SSP5. Individual impacts of ageing on the change in P_{65+UHS} are separated and are compared to those of warming and total population change. The results can provide relative importance of aforementioned phenomena for the change in regional exposure to UHSs, which can be a guideline for planning mitigation policies.

2. Materials and methods

2.1. Definition of summer and the hottest summer

We used the monthly mean temperature of high-resolution gridded datasets from the Climate Research Unit Time Series version 4.03 (CRUTS4) for 1901–2018 as an observation (Harris *et al* 2014). A summer is defined as the hottest season according to records of three consecutive months derived from the 20-year monthly climatology for 1986–2005 at individual grid cells (figure S1 (available online at stacks.iop.org/ERL/15/114043/mmedia)). Further, the summer with the highest temperature during 1901–2018 is defined as the hottest summer. Figure S2 shows the global distribution of the seasonal mean temperature and year of occurrence of the hottest summer over the land surface.

2.2. Projection of UHSs

Seasonal mean temperature during summer is projected using the monthly mean temperature for 1861–2005 and the RCP8.5 scenario for 2006–2100 obtained from 27 GCMs that participated in the fifth phase of the Climate Model Intercomparison Project (CMIP5) (Taylor *et al* 2011; table S1). The first ensemble member of the individual GCMs is interpolated to the half-degree in latitude and longitude and is adjusted to the observation using the bias-correction procedures and observation data from the Climate Prediction Center (see Feng and Fu 2013 for details). The occurrence of UHSs is determined every year for the period of 2006–2100 when the summer mean temperature exceeds the hottest summer temperature based on CRUTS4. The probability of UHSs occurring within 20-year moving windows is computed as the ratio of the number of UHS occurrences within each 20-year period to 20. Each 20-year period is indexed as its final year; thus, the 20-year moving windows for 2006–2100 are from 1987–2006 to 2081–2100. The probability of UHS occurrence is projected at the times when the global mean temperature crosses 1.5, 2, and 3 °C relative to the pre-industrial level ($t_{1.5}$, t_2 , and t_3). Here, $t_{1.5}$, t_2 , and t_3 are calculated as the times whereby the 20-year moving averaged global temperature initially reach 0.9, 1.4, and 2.4 °C above 1986–2005, respectively, because this period was probably, at least, 0.6 °C warmer than the pre-industrial level (Schleussner *et al* 2016, Hawkins *et al* 2017). The mean, 84th and 16th percentile values of the UHS probability of occurrence are calculated based on the spread of 27 GCM projections. Also, the 16%–84% range of the probability of UHS occurrence is computed as the difference between the 84th and 16th percentile values. Note that extreme heat waves, which can induce numerous damages on public health, generally occurred during the recorded hottest summer (Dole *et al* 2011, Steffen *et al* 2017, Yiou *et al* 2020), therefore, the use of UHSs to project exposure of older people in future can be appropriate.

2.3. Projection of POP_{UHS} and P65+_{UHS}

We estimated the total population exposed to UHSs (POP_{UHS}) in six regions, China, India, sub-Sahara countries with low income (SSA-L), Brazil, the US, and the 15 countries that joined European Union prior to 2004 (EU15), at the year of 2040, 2050, and 2070, which are the nearest years to the ensemble median of $t_{1.5}$, t_2 , and t_3 , across 27 GCM simulations (2039, 2052, and 2075), respectively. The gridded dataset of the total population under SSP2, SSP3, and SSP5 for 2010–2100 with a 10-year temporal resolution is considered and interpolated to the half-degree in latitude and longitude (Jones and O’Neil 2016, Fricko *et al* 2017, Fujimori *et al* 2017, Gao 2017, Krieglner *et al* 2017). Both SSP3 and SSP5 can be relevant to the RCP8.5 scenario because these two scenarios are characterised by large emissions from fossil-fuel usage (Riahi 2017). The SSP2 scenario is selected as a middle-of-the-road condition (Riahi 2017). Thus, three SSPs can provide a suitable range of population situations relevant to climate change under the RCP8.5 scenarios. Among the three SSP scenarios, SSP3 and SSP5 show the largest and smallest increase in population with slow and rapid ageing, respectively, and SSP2 represents the middle-of-the-road between SSP3 and SSP5 (table S2; Kc and Lutz 2017). Six regions are selected as those with high populations in individual continents, i.e. East and South Asia, Africa, South and North America, and Europe. The division of regions follows the 32-region level of the SSP database (<https://tntcat.iiasa.acat/SspDb>). For individual regions, the values of POP_{UHS} are estimated as the summation of the population in each grid cell where UHSs occur within the regarding regions (figure S3). Note that population of those six regions represented 61.4% of the world’s population in 2010 (Kc and Lutz 2017).

The projected regional-level population structure dataset under SSP2, SSP3, and SSP5 for 2005–2100 with 5-year discrete temporal resolutions obtained from the SSP database are used to estimate the P65+_{UHS} for 2040, 2050, and 2070 (Kc and Lutz 2017). Initially, the ratio of the P65+ to the total population count (R_{P65+}) is calculated in individual regions. Under an assumption that R_{P65+} is the same for all grid cells within individual regions, P65+_{UHS} is computed as the product of POP_{UHS} and R_{P65+} . Note that this assumption is used to match the gridded population count and regional-level composition of population data.

2.4. Separating individual impacts of warming, population change, and ageing

We calculated the change in P65+_{UHS} in 2070 relative to that in 2040, wherein the global mean temperature exceeded approximately 1.5 °C above the pre-industrial level under the RCP8.5 scenario. The change in the P65+_{UHS} relies on changes in three factors, namely, the UHS occurrence, total

population count, and the ratio of P65+ to total population. The impact of individual factors is designated by impacts of warming (WARM), population change (POP), and ageing (AGEING). Here, we estimated the impact of each factor on the change in the P65+_{UHS} by subtracting the change in the P65+_{UHS}, considering two factors different from all the factors. For example, the impact of POP on the change in the P65+_{UHS} is computed as the difference between the P65+_{UHS} change due to the combined impacts and that due to WARM and AGEING. The estimated impacts of individual factors on P65+_{UHS} can explain which factor causes the change in P65+_{UHS}, as well as the associated potential risks.

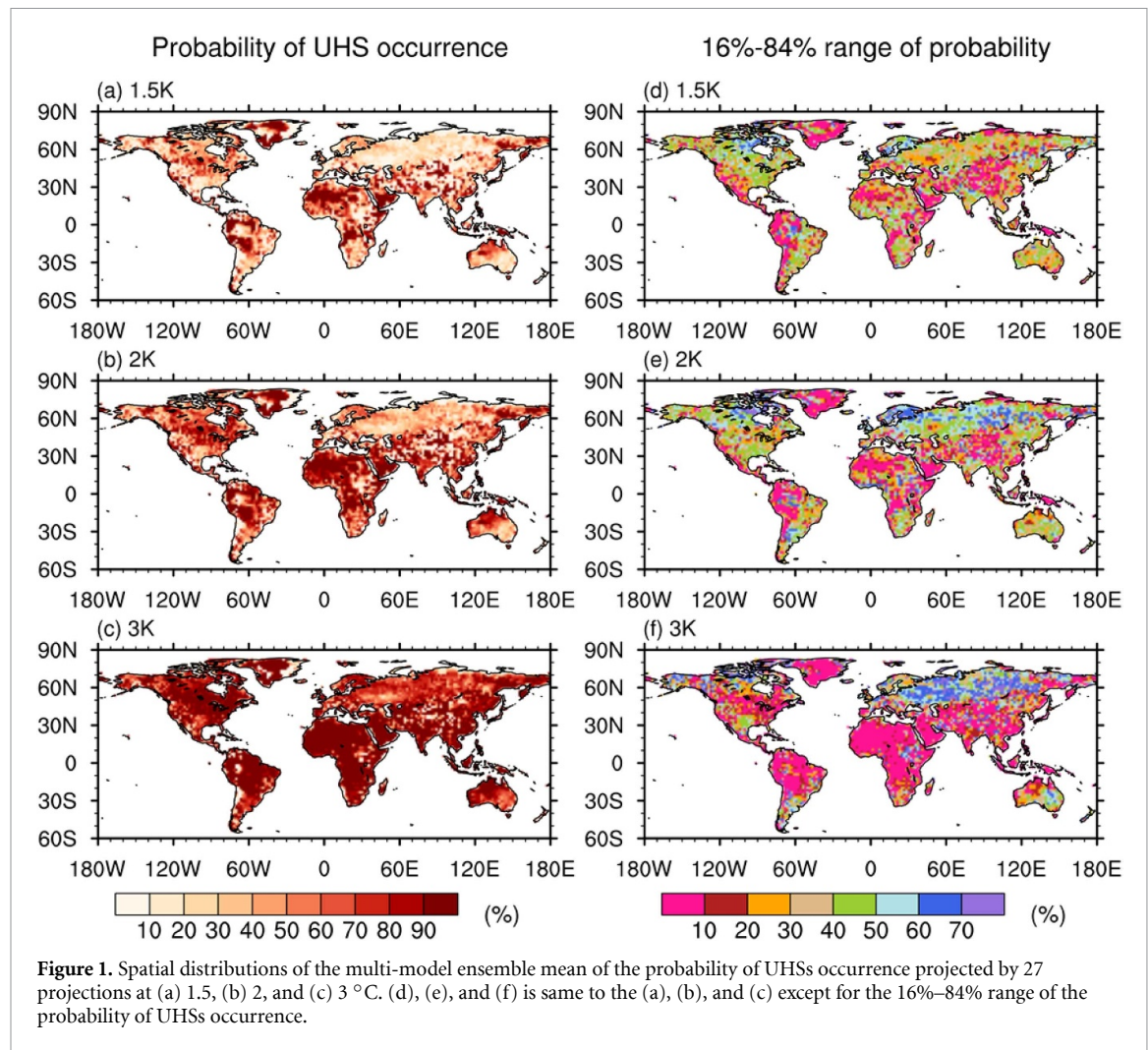
3. Results and discussions

3.1. Projection of UHSs

The multi-model ensemble of probability of UHS occurrence derived from the 27 GCM projections increases with the magnitude of global warming as the summer mean temperature rises (figure 1(a)–(c) and S4). In the 1.5 °C warming scenario, the probability of UHS occurrence shows a distinct regional variation (figure 1(a)). UHSs are likely to occur in many tropical regions, indicating that the people in these regions are at risk of being exposed to UHSs and the associated heat stresses. In contrast, the probability of UHS occurrence is much lower in mid- and high latitudes, except for some regions in North America. This spatial UHS probability of occurrence pattern is connected to the low and high internal variabilities of temperature in the tropics and high latitudes (Harrington *et al* 2016, Lehner *et al* 2018). The probability increases under the 2 °C global warming condition relative to that under the 1.5 °C scenario (figure 1(b)). In particular, the likelihood of UHS occurrence in North America, East Asia, and Southeast Asia shows an increase of more than 30%, whereas the probability is low in Europe, Siberia, and south-eastern Australia. When the global mean temperature reaches 3 °C, the summer mean temperature is likely to exceed the observed record of the hottest summer over almost all of the land surface (figure 1(c)). The regions with high UHS probabilities of occurrence are generally consistent with the areas where the 16%–84% range of UHS probability of occurrence is small, thereby suggesting that the possibility of UHSs occurring is high in those regions (figure 1).

3.2. Total population and P65+ exposed to UHSs

Projecting POP_{UHS} is important for estimating the potential impacts of UHSs on society. In general, more people will experience UHSs in the future due to world population growth, as well as the increase of the probability of UHSs in many areas (Lehner *et al* 2018, Harrington and Friederike 2018). However, the POP_{UHS} can vary by regions and population scenarios. Figure 2 shows the estimated



ensemble median and the 16%–84% range of POP_{UHS} for the population scenario of SSP2, SSP3, and SSP5 across 27 future projections in China, India, SSA-L, Brazil, US, and EU15 at 2040, 2050, and 2070. In China, the POP_{UHS} slightly increases in 2050 relative to that in 2040, and then decreases in 2070 under all population scenarios despite a notable increase in the probability of UHS occurrence because of the decrease in total population since 2030 (figures 1(a)–(c) and 2(a)). In the other five regions, the POP_{UHS} increases under all population scenarios, particularly in SSA-L, according to both the increase in the probability of UHS occurrence and total population (figures 1(a)–(c) and 2(b)–(f)). The change in POP_{UHS} largely varies according to the population scenarios except for China. In India, SSA-L, and Brazil, the increase in the ensemble median of POP_{UHS} under SSP3 reaches 876, 1398, 101 million, which represent a triple, double, and double increase to that under SSP5, respectively (table S3). In contrast, the increment of POP_{UHS} is the largest and smallest under SSP5 and SSP3 in the US and EU15, respectively (figures 2(e) and (f)). The change in POP_{UHS} under the SSP2 scenario lies between that in SSP3 and SSP5 in all regions.

The population structure evolves differently according to regions and population scenarios (Kc and Lutz 2017); thus, temporal changes in $P65+_{UHS}$ are different to those of POP_{UHS} (figures 2 and 3). For all regions, the increasing rate of $P65+_{UHS}$ is larger than that of POP_{UHS} under all SSP scenarios. China shows a large increase in $P65+_{UHS}$, which contrasts the slight change in POP_{UHS} (figures 2(a) and 3(a)). In India, under SSP2, the ensemble median of $P65+_{UHS}$ in 2070 is three times larger than that in 2040, while POP_{UHS} increases by 1.5 times for the same periods (figures 2(b) and 3(b); tables S3 and S4). The $P65+_{UHS}$ in the other four regions are also projected to increase drastically (figure 3(c)–(f)). In addition, the changes in $P65+_{UHS}$ according to individual SSPs are different from those in the POP_{UHS} values in China, India, SSA-L, and Brazil. In these regions, the increase in $P65+_{UHS}$ is the largest and smallest under the SSP5 and SSP3 scenarios, respectively, which is contrary to those in POP_{UHS} (figures 2(a)–(d) and 3(a)–(d)). For example, in India, the increase in the ensemble median of POP_{UHS} in 2070 relative to that in 2040 is 876 million under SSP3, which is three times larger than that under SSP5 (tables S3 and S4). However, for the same period,

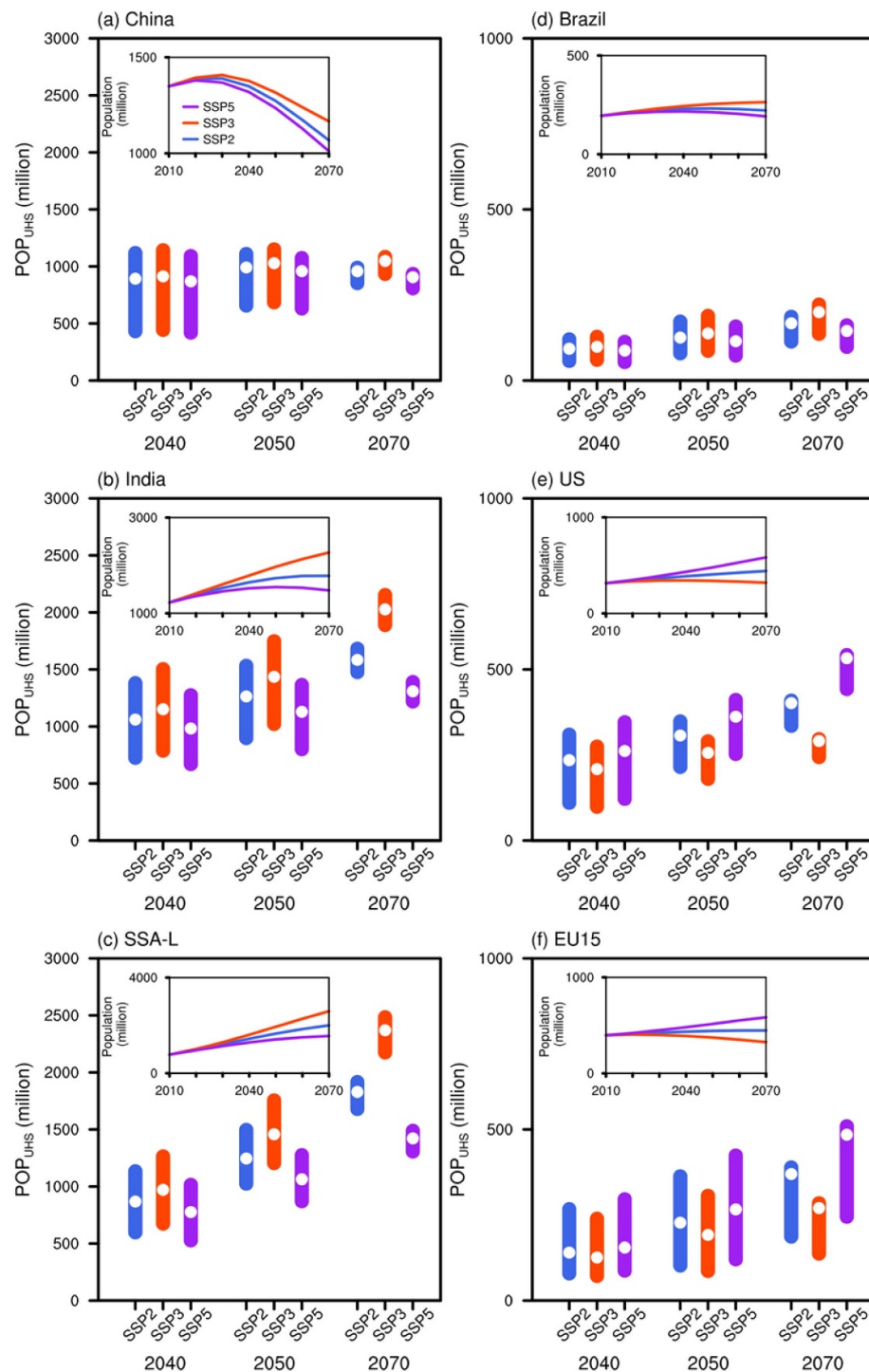


Figure 2. Projected total population for 2010–2070 and POP_{UHS} at 2040, 2050, and 2070 under the SSP2, SSP3, and SSP5 scenarios in (a) China, (b) India, (c) SSA-L, (d) Brazil, (e) US, and (f) EU15. Blue, orange, and purple lines in inner boxes indicate the SSP2, SSP3, and SSP5 scenarios. Blue, orange, and purple bars indicate the 16%–84% percentile ranges of the projections under SSP2, SSP3, and SSP5, respectively. The white dots denote the median of individual projections.

the increase in the ensemble median of $P65+UHS$ in India reaches 173 million under SSP3, which is less than two-thirds of that under SSP5 (tables S3 and S4). Both the US and EU15 show consistent changes in POP_{UHS} and $P65+UHS$ for the three SSPs (figures 2(e), (f), (e), and 3(f)). The contrasting responses of POP_{UHS} and $P65+UHS$ to the population scenarios in China, India, SSA-L, and Brazil are consequent of the distinct evolution of the elderly population to that of

the total population (inner boxes in figures 2 and 3), thereby indicating that ageing should be considered as an important factor for estimating potential risks from heat stresses.

3.3. Driving cause of $P65+UHS$ increase

The change in $P65+UHS$ depends on three factors: (1) increase in UHS occurrence according to warming (WARM), (2) change in total population (POP),

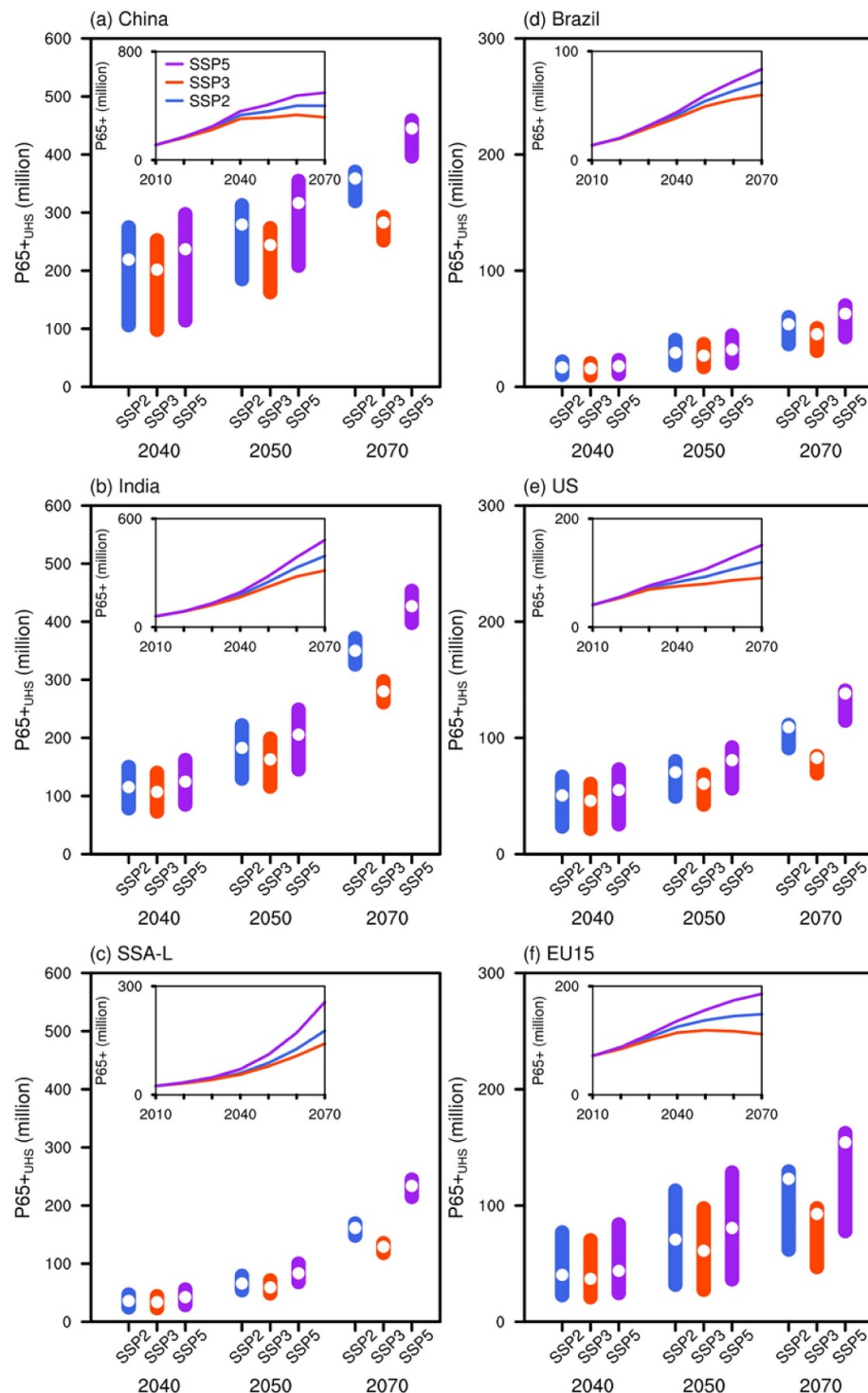


Figure 3. Projected P65+ for 2010–2070 and P65+_{UHS} at 2040, 2050, and 2070 under the SSP2, SSP3, and SSP5 scenarios in (a) China, (b) India, (c) SSA-L, (d) Brazil, (e) US, and (f) EU15. Blue, orange, and purple lines in inner boxes indicate the SSP2, SSP3, and SSP5 scenarios. Blue, orange, and purple bars indicate the 16%–84% percentile ranges of the projections under SSP2, SSP3, and SSP5, respectively. The white dots denote the median of individual projections.

and (3) change in the ratio of P65+ to total population (AGEING). The impacts of WARM, POP, and AGEING on the change in P65+_{UHS} in 2070 relative to that in 2040 are separated to examine the contribution of individual factors, which vary according to regions and population scenarios. Figure 4 shows the projected difference in P65+_{UHS} between 2070 and 2040 according to the combined impacts and

individual factors for all regions and population scenarios. In China, the large increase in P65+_{UHS} results from the WARM and AGEING under all SSP scenarios (figure 4(a)). AGEING is the largest contributor to the increase in P65+_{UHS} in India, SSA-L, and Brazil under population scenarios following SSP2 and SSP5, which represent moderate- and fast-ageing scenarios, respectively (figure 4(b)–(d)). When

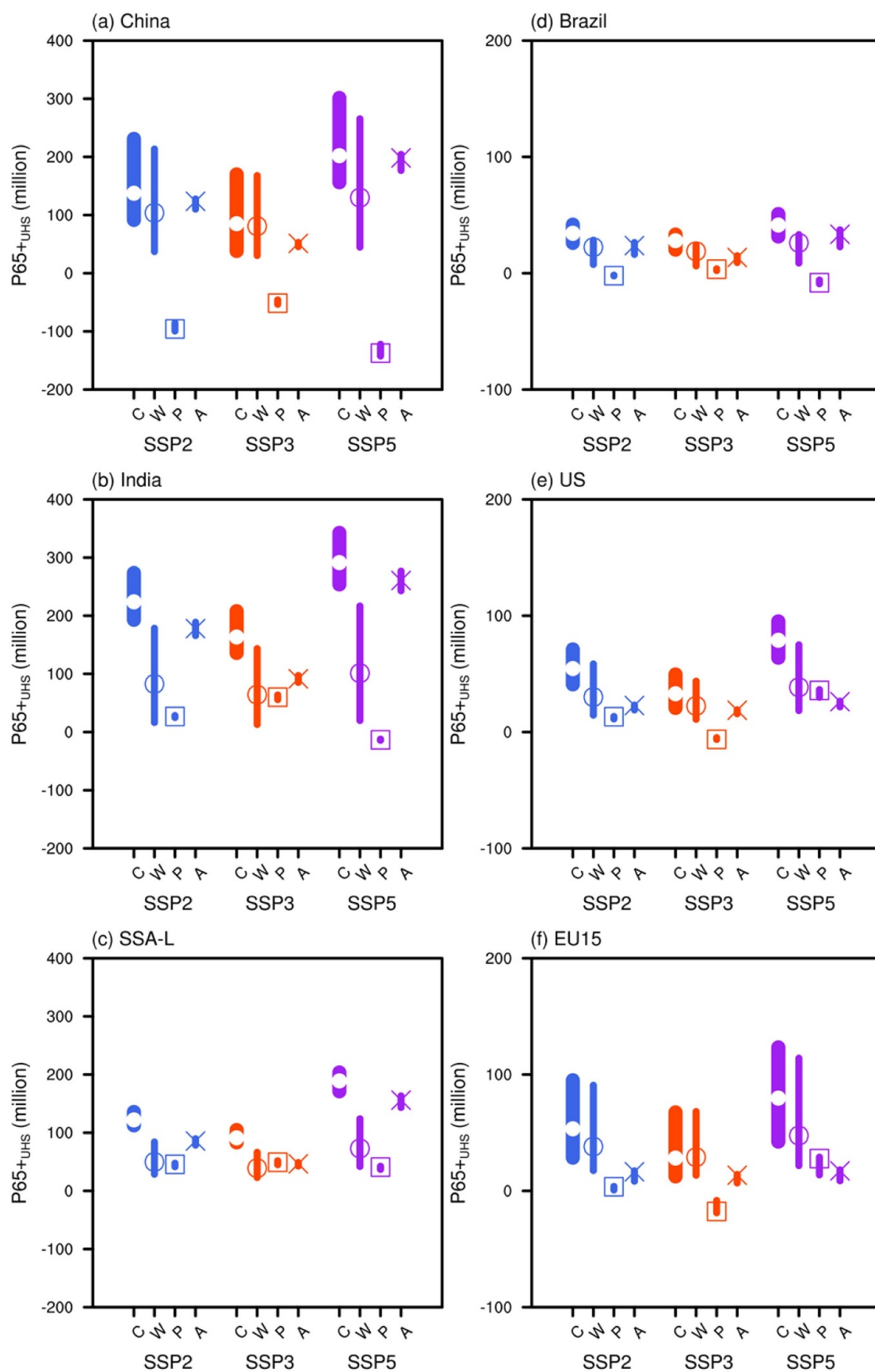


Figure 4. Projected change in $P65+_{UHS}$ in 2070 relative to that in 2040 under SSP2, SSP3, and SSP5 scenarios for (a) China, (b) India, (c) SSA-L, (d) Brazil, (e) US, and (f) EU15. The wide blue, orange, and purple bars indicate the 16%–84% percentile ranges of the projections due to the combined impacts (COMBINE; C) under SSP2, SSP3, and SSP5, respectively. The white dots denote the ensemble median of individual projections. The thin blue bars with circles, squares, and cross markers indicate the 16%–84% percentile ranges and median of projected change under the SSP2 scenarios due to the impact of warming (WARM; W), population change (POP; P), and ageing (AGEING; A), respectively. The thin orange and purple bars with markers are same, but for projections under SSP3 and SSP5 scenarios, respectively.

population change follows the slow ageing scenario SSP3, the combined impacts of the three factors increase P65+_{UHS} in China, India, SSA-L, and Brazil (figure 4(a)–(d)). In the US and EU15, the WARM is the primary reason for the increase in P65+_{UHS} rather than the other considered parameters under all population scenarios (figures 4(e) and (f)). This can be explained by the remarkable increase in the probability of UHS occurrence around 2070, as well as the relatively small change in the total population and P65+ in the US and EU15 relative to that in 2040 (figures 1, 2(e), (f), 3(e), and (f)).

3.4. Discussions

Our results predict that more elderly people will be exposed to heat stresses occasioned by UHSs due to the combined impacts of WARM, POP, and AGEING. Furthermore, the individual contributions of the aforementioned phenomena towards increasing P65+_{UHS} vary by region. In China, India, SSA-L, and Brazil, the ageing-driven increase in P65+_{UHS} in 2070 relative to that in 2040 is larger than the impact of warming and population change, except in the SSP3 scenario (figure 4(a)–(d)). This indicates that the potential impacts of UHSs on public health will increase due to ageing in those regions even if we limit global warming to the level in 2040, comparable to 1.5 °C above the pre-industrial level. In addition, the health risks resulting from warming and ageing may be amplified in the aforementioned regions due to the relatively deficient economic capabilities (Harrington *et al* 2016). Thus, the economic support of developed countries is necessary for developing regions to establish age-friendly health and social services to mitigate the threat of UHSs to the aged societies of the future. In contrast, in both the US and EU15, the growth in P65+_{UHS} according to warming and the associated increase in the probability of UHS occurrence is much larger than that due to the change in other factors under all population scenarios (figures 4(e) and (f)). In addition, the regulated strength of UHSs under a target warming level, such as a 1.5 °C warming relative to the pre-industrial period, can suppress heat stresses in other regions that experience rapid ageing (King *et al* 2018, Lehner *et al* 2018). Efforts on traditional mitigation strategies that focus on reducing the emission of greenhouse gases and the relevant global warming effects are essential to reduce health problems associated with unprecedented summer heat in an aged society.

Acknowledgments

This work was supported by the Korea Meteorological Administration Research and Development Program under Grant KMI(KMI2020-01118), and Creative-Pioneering Researchers Program through Seoul National University (SNU). Additional support

was provided by National Natural Science Foundation of China (Grant No. 41890852).

Data availability statement

The data that support the findings of this study are available upon reasonable request from the authors. High-resolution gridded data sets provided by the Climate Research Unit for this research are available in the following in-text data citation references: Harris *et al.* (2014) (<https://crudata.uea.ac.uk/cru/data/hrg/>). Bias-corrected 27 GCM climate projections for this research are included in this paper: Feng and Fu (2013). The gridded dataset of total population following SSP scenarios are available in the following in-text data citation references: Jones and O'Neil (2016) (<http://www.cgdr.ucar.edu/iam/modeling/spatial-population-scenarios.html>). Regional level composition of population under SSP scenarios are available through SSP public database in the following in-text data citation references: Kc and Lutz (2017) (<https://tntcat.iiasa.ac.at/SspDb/>).

Competing interests

The authors declare no competing financial interests.

ORCID iDs

Chang-Eui Park  <https://orcid.org/0000-0001-8792-6778>
Sujong Jeong  <https://orcid.org/0000-0003-4586-4534>
Luke J Harrington  <https://orcid.org/0000-0002-1699-6119>
Myong-In Lee  <https://orcid.org/0000-0001-8983-8624>
Chunmiao Zheng  <https://orcid.org/0000-0001-5839-1305>

References

- Arnell N W, Brown S, Gosling S N, Hinkel J, Huntingford C, Lloyd-Hughes B, Lowe J A, Osborn T, Nicholls R J and Zelazowski P 2016 Global-scale climate impact functions: the relationship between climate forcing and impact *Clim. Change* **134** 475–87
- Baccini M, Kosatsky T, Analitis A, Anderson H R, D'Ovidio M, Menne B, Michelozzi P and Biggeri A 2011 Impact of heat on mortality in 15 European cities: attributable deaths under different weather scenarios *J. Epidemiol. Community Health* **65** 65–79
- Basu R 2009 High ambient temperature and mortality: a review of epidemiologic studies from 2001 to 2008 *Environ. Health* **8** 40
- Dole R, Hoerling M, Perlwitz J, Eischeid J, Pegion P, Zhang T, Quan X-W, Xu T and Murray D 2011 Was there a basis for anticipating the 2010 Russian heat wave? *Geophys. Res. Lett.* **38** L06702
- Feng S and Fu Q 2013 Expansion of global drylands under a warming climate *Atmos. Chem. Phys.* **13** 10081–94

- Fricko O *et al* 2017 The marker quantification of the shared socioeconomic pathway 2: a middle-of-the-road scenario for the 21st century *Global Environ. Change* **42** 251–67
- Fujimori S, Hasegawa T, Masui T, Takahashi K, Herran D S, Dai H, Hijioka Y and Kainuma M 2017 SSP3: AIM implementation of shared socioeconomic pathways *Global Environ. Change* **42** 268–83
- Gao J 2017 *Downscaling Global Spatial Population Projections from 1/8-degree to 1-km Grid Cells* NCAR Technical Note NCAR/TN-537+STR
- Guo Y *et al* 2017 Quantifying excess deaths related to heatwaves under climate change scenarios: a multicountry time series modelling study *PLoS Med.* **15** e1002629
- Hajat S *et al* 2010 Heat–health warning systems: a comparison of the predictive capacity of different approaches to identifying dangerously hot days *Am. J. Public Health* **100** 1137–44
- Harrington L J, Frame D J, Fischer E M, Hawkins E, Joshi M and Jones C D 2016 Poorest countries experience earlier anthropogenic emergence of daily temperature extremes *Environ. Res. Lett.* **11** 055007
- Harrington L J and Friederike E L O 2018 Changing population dynamics and uneven temperature emergence combine to exacerbate regional exposure to heat extremes under 1.5 °C and 2 °C of warming *Environ. Res. Lett.* **13** 034011
- Harris I, Jones P D, Osborn T J and Lister D H 2014 Updated high-resolution grids of monthly climatic observations – the CRU TS3.10 Dataset *Int. J. Climatol.* **34** 623–42
- Hawkins E *et al* 2017 Estimating changes in global temperature since the pre-industrial period *Bull. Am. Meteorol. Soc.* **98** 1841–56
- Jones B and O’Neil B C 2016 Spatially explicit global population scenarios consistent with the Shared Socioeconomic Pathways *Environ. Res. Lett.* **11** 084003
- Jones B, O’Neill B C, McDaniel L, McGinnis S, Mearns L O and Tebaldi C 2015 Future population exposure to US heat extremes *Nat. Clim. Change* **5** 652–5
- Kc S and Lutz W 2017 The human core of the shared socioeconomic pathways: population scenarios by age, sex and level of education for all countries to 2100 *Global Environ. Change* **42** 181–92
- Kenney W L and Munce T A 2003 Invited review: aging and human temperature regulation *J. App. Physiol.* **95** 2598–603
- King A D 2017 Attributing changing rates of temperature record breaking to anthropogenic influences *Earth’s Future* **5** 1156–68
- King A D, Donat M G, Lewis S C, Henley B J, Mitchell D M, Stott P A, Fischer E M and Karoly D J 2018 Reduced heat exposure by limiting global warming to 1.5 °C *Nat. Clim. Change* **8** 549–51
- Kriegler E *et al* 2017 Fossil-fueled development (SSP5): an energy and resource intensive scenario for the 21st century *Global Environ. Change* **42** 297–315
- Larrieu S, Carcaillon L, Lefranc A, Helmer C, Dartigues J-F, Tavernier B, Ledrans M and Filleul L 2008 Factors associated with morbidity during the 2003 heat wave in two population-based cohorts of elderly subjects: PAQUID and Three City *Eur. J. Epidemiol.* **23** 295–302
- Lehner F, Deser C and Sanderson B M 2018 Future risk of record-breaking summer temperatures and its mitigation *Clim. Change* **146** 363–75
- Li T *et al* 2016 Aging will amplify the heat-related mortality risk under a changing climate: projection for the elderly in Beijing, China *Sci. Rep.* **6** 28161
- Mather M, Jacobsen L A and Pollard K M 2015 *Aging in the United States* Population Reference Bureau
- Riahi K 2017 The Shared Socioeconomic Pathways and their energy, land use, and greenhouse gas emissions implications: an overview *Global Environ. Change* **42** 153–68
- Schleussner C-F, Rogelj J, Schaeffer M, Lissner T, Licker R, Fischer E M, Knutti R, Levermann A, Frieler K and Hare W 2016 Science and policy characteristics of the Paris agreement temperature goal *Nat. Clim. Change* **6** 827–35
- Statistical Office of the European communities 1990 *EUROSTAT: regional Statistics.: reference Guide* Luxembourg, Eurostat, Graphical information available at <https://ec.europa.eu/eurostat/cache/infographs/elderly/index.html> (Assessed: 5 May 2020)
- Steffen W, Stock A, Alexander D and Rice M 2017 *Angry Summer 2016/17: climate change super-charging extreme weather* Climate Council of Australia
- Taylor K E, Stouffer R J and Meehl G A 2011 An overview of CMIP5 and the experiment design *Bull. Am. Meteorol. Soc.* **93** 485–98
- United Nations 2019a *World Population Prospects 2019: highlights* Department of Economic and Social Affairs, Population Division
- United Nations 2019b *World Population Ageing 2019: highlights (ST/ESA/SER.A/430)* Department of Economic and Social Affairs, Population Division
- Urban A, Hanzlíková H, Kyselý J and Plavcová E 2017 Impacts of the 2015 heat waves on mortality in the Czech republic—a comparison with previous heat waves *Int. J. Environ. Res. Public Health* **14** 1562
- Urban A, Kyselý J, Plavcová E, Hanzlíková H and Štěpánek P 2020 Temporal changes in years of life lost associated with heat waves in the Czech Republic *Sci. Total Environ.* **716** 137093
- World Health Organization (WHO) 2011 *Global health and ageing* US National Institute of Aging, World Health Organization
- World Health Organization (WHO) 2015a *World report on ageing and health* WHO Press, World Health Organization
- World Health Organization (WHO) 2015b *China country assessment report on ageing and health* WHO Press, World Health Organization
- Yiou P *et al* 2020 Analyses of the Northern European summer heatwave of 2018 *Bull. Am. Meteorol. Soc.* **101** S35–S40